OSJ | OPEN SCIENCE JOURNAL

RESEARCH ARTICLE

# Winter Beans: the Use of an Unmanned Aerial Vehicle for Monitoring and Prediction of Crop Performance

Shara Ahmed[1], Catherine E. Nicholson[1], Simon R. Rutter[1], John R. Marshall[1], Justin J. Perry[1], John R. Dean[1*]

[1]Northumbria University, Department of Applied Sciences, Newcastle upon Tyne, NE1 8ST, United Kingdom

*Corresponding author: John R. Dean: John.Dean@northumbria.ac.uk

OPEN ACCESS

Citation: Ahmed S., Nicholson C.E., Rutter S.R., Marshall J.R., Perry J.J., Dean J.R. (2023) Winter Beans: the Use of an Unmanned Aerial Vehicle for Monitoring and Prediction of Crop Performance. Open Science Journal 8(2)

Received: 11th January 2023

Accepted: 17th April 2023

Published: 25th May 2023



Funding: The author(s) received no specific funding for this work

Competing Interests: The authors have declared that no competing interests exists.

## Abstract:

Traditional field-based techniques for phenotyping of crops are based on visual assessment which are subjective and time consuming. A high throughput automated technique using an unmanned aerial vehicle (UAV) with a multispectral image (MSI) camera was used to investigate the correlation between markers of winter bean crop development with eventual crop yield. A simplified approach has been developed using different vegetation indices i.e. NDVI, GNDVI and NDRE, coupled with an iso-cluster classification method to monitor plant characteristics across all growing stages. The UAV-MSI data could then be incorporated into a yield estimator model to estimate the winter bean seed yield. The NDVI approach showed the greatest correlation between the modelled seed yield and the actual seed yield determined on two separate occasions ($R^2 = 0.84$ and $R^2 = 0.87$). In addition, GNDVI and NDRE were a better estimator of seed yield for areas with dense vegetation. These are hence shown to be able to monitor a winter bean harvest in an efficient and timely manner.

Keywords: Winter beans, Unmanned aerial vehicle, Multispectral imaging, Crop yield prediction, Phenotyping

## Introduction

Winter bean is a widely cultivated crop worldwide consumed as both food and animal feed (1). The total UK bean production varies between 500,000 to 600,000

tonnes per year (2). Typically, around 150,000 tonnes of beans are exported globally for human consumption and the remainder is sold locally (2). Annual demand of beans for animal feed in the UK ranges between 270,000 to 350,000 tonnes (2). According to data from the processors growers research organisation (PGRO) in the UK the leading varieties of winter bean are Vincent, Vespa, Bumble, Norton, Wizard, Honey, and Tundra (3). Tundra is the highest yielding variety on the PGRO winter bean recommended list as it has a high protein content making it suitable for export market, human consumption, and animal feed (3). However, as for all crops, disease, weed growth, and adverse weather conditions can significantly influence the winter bean crop yield (4). This makes it challenging to meet the growing demand for winter beans on the global market. Hence, the requirement for an efficient crop management and monitoring system needs to be implemented.

The phenological growth stages of winter bean is shown in Figure 1 (5) Stage 1 and 2 involves seed germination and stem elongation. Stage 3 and 4 involves flowering and pod development. Finally, stage 5 incorporates pod ripening and senescence. Plant phenotyping systems can be used to unravel the phenotypic traits across different phenological growth stages for effective management of crops. Ground based methods of quantifying crop biomass across growth stages involves cutting, drying, and weighing of crops collected from a target area (6). Ground based methods are however invasive to the crop and there is a limit to the number of samples that can be collected from a plot. This has led to the development of plant phenotyping using non-invasive imaging techniques by remote sensing. Typically, remote sensing requires a higher spatial resolution of 1-3 m for crop yield estimation and a spatial resolution of 5 - 10 m for nutrient management (7). Whereas weed mapping requires a finer spatial resolution of 5 - 50 cm to effectively identify weed patches around crops. Even though satellites can provide high spatial (5 m) and temporal (daily) resolution images, most publicly available satellite products have coarse resolution for many precisions agricultural applications (8). In comparison, the deployment of unmanned aerial vehicle (UAV) platforms can typically provide much lower spatial resolution (<5 m), making them suitable for effective precision agricultural applications.

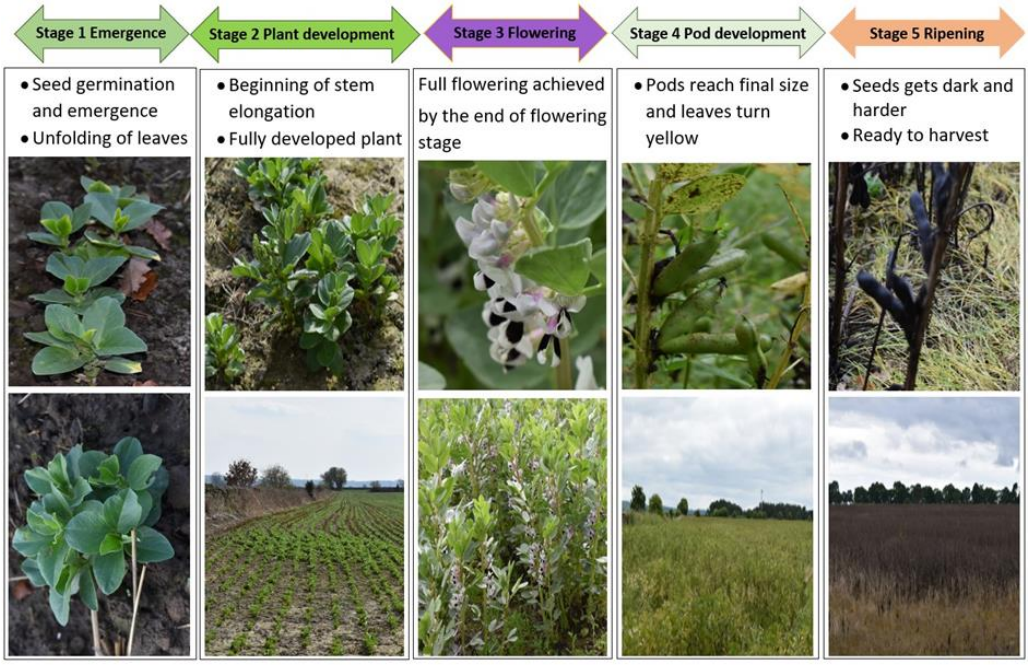


Figure 1. Phenological growth stages of winter beans.

Only a limited number of studies using remote sensing platforms have focused on different bean types. A recent study, using a UAV, monitored both the growth of the faba bean across the phenological growth stages and using machine learning algorithms estimated the yield of faba bean (9). Soybeans have been the focus of a few studies. A UAV-MSI has been deployed to predict soybean yield based on vegetation indices coupled with machine learning regression models (10) and soyabean yield has been predicted, from UAV-MSI data, using a deep learning method (11). Our study focuses on investigating the crop development across five phenological growth stages of winter beans (Tundra) to assess their final yield using a UAV-MSI approach.

Data collected by a UAV-MSI can be interrogated using various vegetation indices. The normalised difference vegetation index (NDVI) and the green NDVI have been used to determine crop biomass, yield and photosynthetic activity (8). While the normalised difference red edge (NDRE) measure has been reported to be more sensitive in estimating crop biomass in dense vegetation in comparison to NDVI (12). Consequently, we have used NDVI, GNDVI and NDRE to predict winter bean seed yield based on data from the flowering stage of crop plants (Figure 1). Processing of the UAV-MSI data to assess the vegetation indices has been done using the simpler and precise image classification method of iso-clustering. Iso-clustering classification is an automated unsupervised classification model that aims to segment similar clusters to groups by assigning distinctive pixel values in a manner similar to k-means clustering but is more automated and precise. In this study a previously developed crop estimation model (13) is used to count the number of leaf pixels by the iso-cluster approach to estimate the yield. In this way we demonstrate how to estimate the winter bean seed yield at the early flowering stage for the first time.

The aims of the research are (a) to evaluate the performance of a UAV-MSI camera to estimate winter bean crop development across the different phenological growth stages over an 11 month growth cycle, (b) to predict the final winter bean seed yield (in mid-August) using NDVI, GNDVI and NDRE coupled with an iso-cluster classification method, during the flowering stage (May), and (c) to assess the accuracy of each vegetation index to predict the seed yield.

## Materials and Methods

### *Airy Holme farm*

Winter bean seed (variety, Tundra) was planted at a rate of 220 kg / hectare using a Claydon Hybrid T4 trailed drill (Rickerby, Hexham, UK) pulled by a Claas ARES 836 RZ tractor (Rickerby, Hexham, UK) to a depth of 70 mm on the 29 September 2020 in a 5.29 hectare field (Lat. 54.88038; Long. -1.87972), known locally as High Dowell. The field was treated as follows in general terms, for protection of the winter bean crop: Within a week of the sowing date (early October), a specific herbicide was applied to the soil prior to crop and weed emergence (Clomate®, Albaugh Europe, Lausanne, Switzerland) alongside Most Micro, a pendimethalin herbicide, used for the control of annual grass and broadleaved weeds (Most Micro, Sipcam (UK) Ltd., Royston, Herts). In (early December) a foliar acting selective herbicide with systemic activity on a wide range of grass weeds and volunteer cereals (Falcon®, Adama Agricultural Solutions UK

Ltd, Reading) was applied. A broad-spectrum systemic fungicide (Custodia, Adama Agricultural Solutions UK Ltd, Reading) was applied in early June. Finally, 21 days prior to harvesting of the winter bean crop a pre-harvest desiccate was applied (Roundup Vista plus, Bayer Crop Science, Cambridge, UK). The addition of a desiccate assists in producing an evenly ripe crop (and eliminates perennial weeds) to aid harvesting.

To promote growth of winter beans fertilizer, NPK(S), 20-8-12($7SO_3$) with the composition: total nitrogen (N) of which nitric nitrogen (9.2%) and ammoniacal nitrogen (10.8%); phosphorus pentoxide soluble in neutral ammonium citrate and in water ($P_2O_5$) 8% (3.5% P) of which phosphorus pentoxide soluble in water ($P_2O_5$) 7.7% (3.3% P); potassium oxide soluble in water ($K_2O$) 12% (10% K); sulfur trioxide soluble in water ($SO_3$) 7% (2.8% S) (CF Fertilisers UK Ltd., Billingham, UK) was applied at the time of sowing (29 September 2020). Additional nutrients were also added in spring (April) and included supplements for boron, manganese and molybdenum (Lebosol® Rapsmix SC, Lebosol® Dunger GmbH, Elmstein, Germany), phosphate, potassium and magnesium (Yaravita Magphos K, Yara Ireland, Grimsby, UK) and, in June, phosphorus and calcium (Calfite extra, Agrovista UK Ltd., Nottingham, UK). In addition, an adjuvant, Boost (Dow Agro Sciences, King's Lynn, UK) was added to assist with ground coverage, soil penetration, crop uptake and rainfastness.

### *High Dowell agricultural field*

Soil analysis was done on this agricultural field in March 2021 and data reported on the 15 March 2021 (by Lancrop Laboratories, Pocklington, UK in association with Agrovista UK Ltd., Nottingham, UK). Soil analysis indicated the following characteristics, a sandy loam (sand 52.5%; silt 40.1%, and 7.4%) with a pH of 7.6, organic matter (4.0%) and a cation exchange capacity of 15.1 meq/100 g had a high level of the major nutrient i.e. phosphorus (33 ppm) against a guideline value of 26 ppm. A normal level of potassium (164 ppm) against a guideline value of 241 ppm, and deficient in magnesium (44 ppm) against a guideline value of 50 ppm. For secondary and micronutrients maintenance levels were noted for calcium (3006 ppm) against a guideline value of 1600 ppm, copper (3.3 ppm) against a guideline value of 2.1 ppm, iron (687 ppm) against a guideline value of 50 ppm, and zinc (6.2 ppm) against a guideline value of 2.1 ppm. However, deficiencies were noted in term of secondary and micronutrients, specifically, sulfur (2 ppm) against a guideline value of 10 ppm; sodium (17 ppm) against a guideline value of 90 ppm; boron (1.2 ppm) against a guideline of 1.6 ppm; manganese (32 ppm) against a guideline of 100 ppm; and molybdenum (0.07 ppm) against a guideline of 0.2 ppm. For the winter bean crop advice was provided that indicated that treatment with the following was required magnesium (major nutrient), sulfur, boron, manganese and molybdenum. Therefore, supplements were added to the field to rectify these deficiencies. The desiccated crop was harvested on the 1 September 2021 using a Claas Lexion 570, Terra-Trac combine harvester (Rickerby, Hexham, UK). The seed is monitored by sensors (FarmTRX, Troo Corp., Ottawa, Canada), which record both the yield, and its location using GPS technology, into an on-board data logger.

### *Unmanned aerial vehicle*

A multirotor UAV (DJI Phantom 4, supplied by Coptrz Ltd., Leeds, UK) was used with a multispectral camera with a 5 camera-array covering the blue (450 ± 16 nm), green (560 ± 16 nm), red (650 ± 16 nm), red edge (730 ± 16 nm) and near-infrared (840 ± 26 nm) spectra with an additional camera that can also provide live images in RGB (visible) mode as well as in normalized difference vegetation index (NDVI) mode. All cameras were stabilized with a 3-axis gimbal. In all cases, the camera was angled perpendicular to the ground, with data capture occurring in hover and capture mode. Images (1548 image files per flight gathered over 256 waypoints) were captured as 16-bit TIF files corrected for ambient radiance values. The UAV speed was 5.0 m/s and had an average height of 50.6 m for the 2901 m flight distance. All flights were recorded with a resolution of 2.7 cm/px, a front overlap ratio of 75%, a side overlap ratio of 60% and a course angle of 90°. Specific weather conditions relating to daytime temperature during flight, wind speed and direction (recorded using a handheld anemometer (Benetech® GM816, Amazon UK)), and UAV pilot anecdotal observations on cloud coverage are identified with specific dated data.

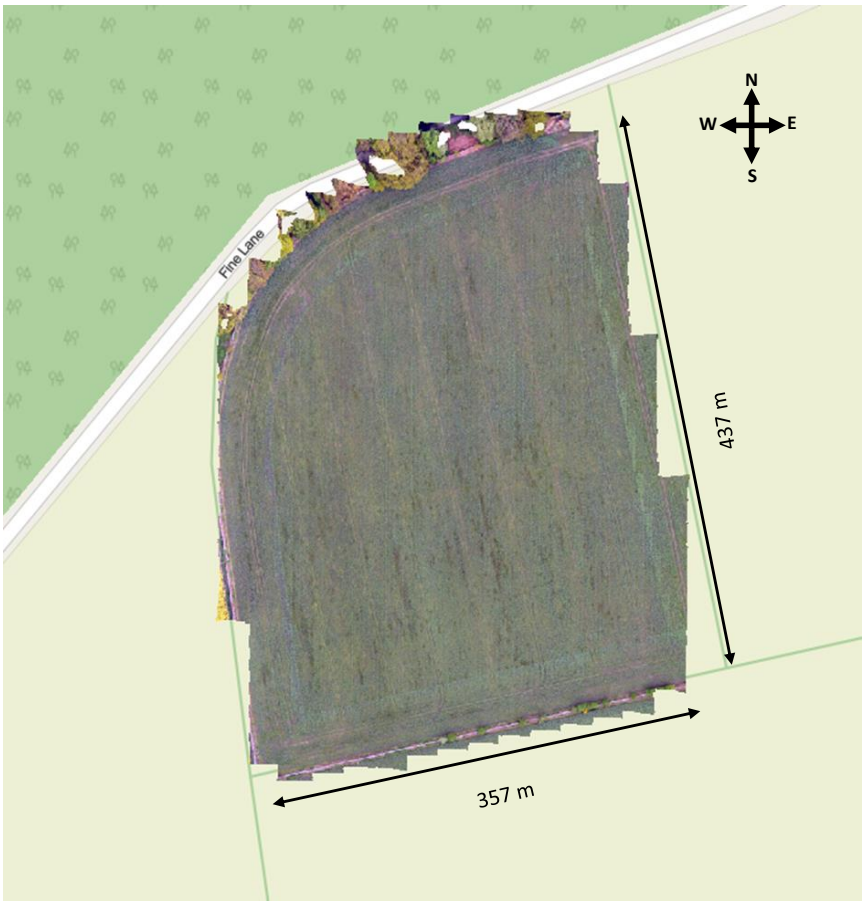


Figure 2. Orthomosaic image of High Dowell: winter bean field, with an area of 5.29 ha.

### *Crop development*

An estimation of the height of the winter bean crop, across the phenological growth stages, was performed on ArcGIS Pro v.2.8.0 software (Esri Inc., West Redlands, CA, USA). ArcGIS Pro software generates a canopy height model (CHM) based on the concept of structure from motion (SfM) principle. The SfM photogrammetry creates a rigid 3D model by matching similar features of several overlapping images (14). The 3D point clouds built by Agisoft were extracted and used by ArcGIS Pro to create CHMs based on time-series data linked to the winter bean phenological growth stages (Figure 3). The 3D points were initially used to create a digital surface model (DSM) and a digital terrain model (DTM). The DSM is calculated by including features elevated above ground, whereas the DTM is calculated by interpolating features from ground or soil surfaces. The DSM and DTM for each spectral band were combined to create a multispectral raster image. The CHM, which is the height between the ground and the top of the winter bean crop was then calculated in ArcGIS using the raster calculator tool (CHM = DSM - DTM). Finally, to extract winter bean height from a specific region, a polygon was drawn outlining the field. In this manner the height of winter bean crop was extracted across different phenological growth stages.

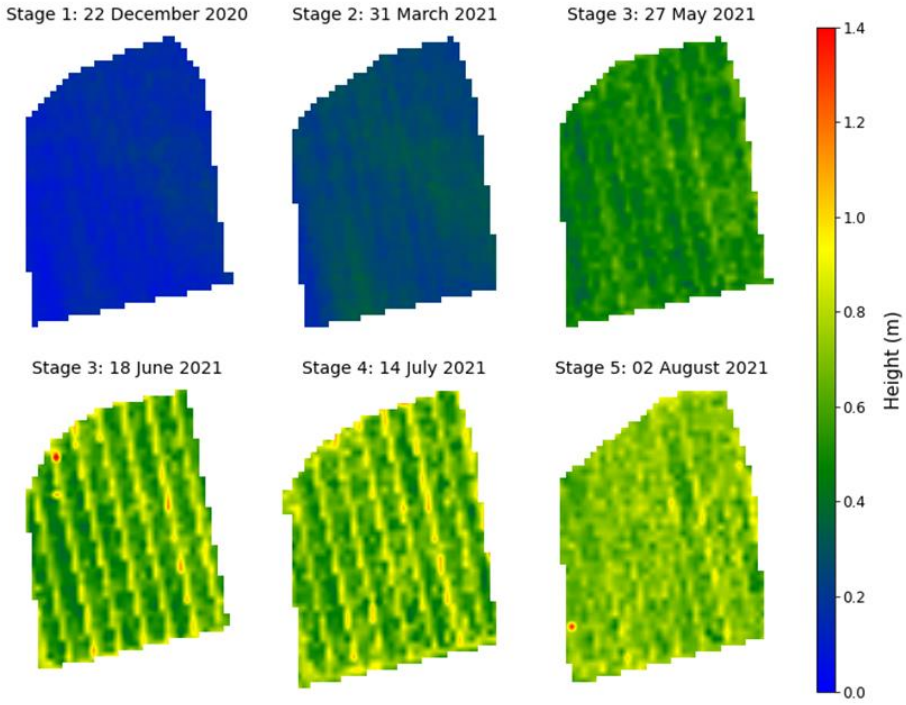


Figure 3. 3D Canopy height model of winter bean at different phenological growth stages.

### *Vegetation index calculation and iso-cluster classification*

ArcGIS Pro software was used for vegetation index calculation and iso-cluster classification. The raster calculator tool in ArcGIS was used to generate specific vegetation index maps by applying three vegetation indices, NDVI, GNDVI, and NDRE, to multispectral data. The NDVI spectral index was calculated by measuring the difference between the NIR and red spectral bands (15), GNDVI was calculated by measuring the difference between NIR and green spectral bands (16), and NDRE was calculated by measuring the difference between NIR and deep red spectral bands (17).

$$\text{NDVI} = \frac{(\text{NIR}-\text{Red})}{(\text{NIR}+\text{Red})} \quad (1)$$

$$\text{GNDVI} = \frac{(\text{NIR}-\text{Green})}{(\text{NIR}+\text{Green})} \quad (2)$$

$$\text{NDRE} = \frac{(\text{NIR}-\text{Deep Red})}{(\text{NIR}+\text{Deep Red})} \quad (3)$$

The vegetation indices were calculated on two gathered image datasets of the same field at two different dates during flowering in May (14 and 27 May) 2021. Vegetation index maps underwent iso-cluster classification. In ArcGIS Pro, iso-cluster classification is an unsupervised classification tool that automatically groups similar clusters to produce a classified image. It works on the same principle as k-means clustering, with centroids placed based on the number of clusters assigned. The Euclidian distance between each pixel and its centroid was calculated. The pixels for each cluster were classified into separate clusters based on their closest Euclidian distance, with each cluster having a similar value. Six clusters were assigned to classify the vegetation index maps. The first cluster had pixels representing the soils surface, while the second cluster include pixels representing grasslands or shrubs. The remaining four clusters represented healthy vegetation index values between 0.4 – 1.0 in the winter bean crop and these were classified together.

### *Winter bean seed yield estimation*

A simplified pixel-based approach (as originally proposed by (13)) was used to segregate healthy vegetation pixels in the winter bean crop to estimate the seed yield, in units of t/ha, using the following equation:

$$\text{Estimated seed yield (t/ha)} = \frac{F \; x \; P(beans)}{A} \quad (4)$$

Where, F is the weighting factor to scale the relationship. The higher the F value, the higher the crop yield. The value for F is determined as follows: F = healthy vegetation pixels / $\Sigma$ pixels; P(beans) = area ($m^2$) of healthy vegetation pixels in the field. This is calculated by multiplying the number of pixels of healthy vegetation by the resolution of the drone images (i.e. (0.027 m / pixel)$^2$) in tonnes; and A = Area of the field (ha).

According to the actual corrected seed yield map (Figure 4), supplied by FarmTRX (Troo Corp., Ottawa, Canada), some variation of yield is noted across the 5.29 ha of field area. The yield map has variation across its area, highlighted as follows: A. low yield (red with minimum = 0 t/ha, mean = 1.15 t/ha and maximum = 1.21t/h); B. medium (orange with minimum = 1.21 t/ha, mean = 1.28 t/ha and

maximum = 1.33 t/h); C. high (yellow with minimum = 1.33 t/ha, mean = 1.38 t/ha and maximum = 1.42 t/h); and, D. very high (green with minimum = 1.4 t/ha, mean = 1.57 t/ha and maximum = 1.9 t/h) yield areas (Figure 4). As a result, and with reference to the corrected yield map (FarmTRX), the predicted seed yield based on the vegetation index map by iso-cluster image was determined in 25 distinct points within High Dowell for the four identified yield states (i.e. low, medium, high and very high).

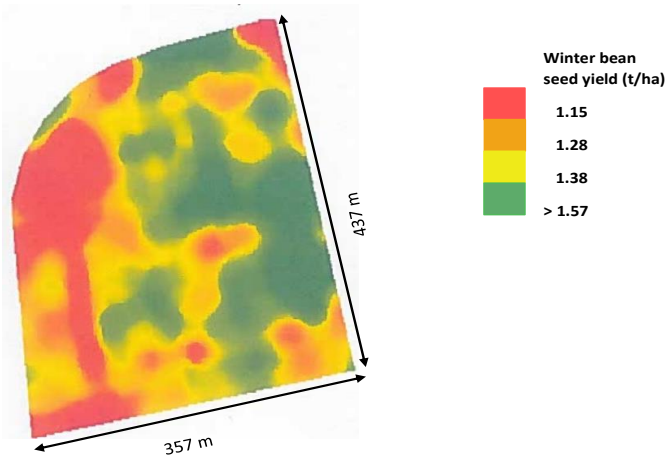


Figure 4. Actual yield map of winter bean seed yield
(Note: The reported field area is 5.29 ha (or 52,900 $m^2$)

## *Statistical analysis*

To analyse the link between the estimated seed yield and the actual yield, Pearson correlation and root mean square error (RMSE) calculations were made. The larger $R^2$ and low RMSE will indicate the higher precision and accuracy of the estimated yield model.

$$\text{RMSE} = \frac{\sqrt{\sum_{i=1}^{n}(yi-\widehat{yi})}}{(n)} \qquad (5)$$

where $yi$ = estimated yield; $\widehat{yi}$ = actual yield; and $n$ = number of observations.

## Results and Discussion

### *Estimation of winter bean development across the phenological growth stages.*

The height of the winter bean crop in High Dowell (5.29 ha) across the phenological growth stages was estimated using the CHM. To corroborate the canopy height data of winter beans using UAV-MSI data treatment, ground truth data was obtained by measuring the height of the wall used as a boundary to the east of the field and compared with UAV-MSI estimated data. The manually measured wall heights (1.07 ± 0.04 m, n = 3) compared favourably with the UAV-MSI CHM estimated wall height (1.00 ± 0.11, n = 3, as determined on three different days) using statistical analysis (t-test). The t-test results indicated a p-value of 0.17 at the 95% confidence interval. It was therefore concluded that there was no statistically significant difference between the two measurements (ground truth versus UAV-MSI CHM data), hence the accuracy of using the UAV-MSI CHM approach was confirmed. For this reason and to aid the automation desirable for this method's utility, the estimated winter bean plant height measurements, estimated from UAV-MSI CHM, were used uncorrected for the rest of the study.

A boxplot illustrating the phenological growth stages of winter beans from December 2020 to August 2021 is shown in Figure 5. In stage 1 (emergence), the mean winter bean height is 0.14 m (minimum 0.046 m and maximum 0.24 m). In stage 2 (plant development), the mean winter bean height is 0.27 m (minimum 0.11 m and maximum 0.37 m. In stage 3 (flowering), the mean winter bean height is 0.60 m (minimum 0.30 m and maximum 0.82 m). In stage 4 (pod development), the mean winter bean height is 0.60 m (minimum 0.27 m and maximum 1.0 m). Finally, in stage 5 (ripening), the mean winter bean height is 0.71 m (minimum 0.37 m and maximum 1.2 m). The results from the study (Figure 5) indicate a steady increase in winter bean plant height until the final stage 5 of ripening. The biggest growth in plant height occurs between stages 2 (plant development) and 3 (flowering) where the average plant height has increased by nearly 33% from 0.27 m to 0.6 m (Figure 5). This growth was probably facilitated by the addition of advised nutrients, boron, magnesium, manganese, molybdenum, as well as phosphate and potassium, to the soil. Further, between stage 3 (Flowering) until stage 5 (Ripening) there was only a slight increase of average winter bean plant height by 10% from 0.6 m to 0.7 m (Figure 5) as plant growth slows down after the flowering stage in preparation for pod development and ripening. The maximum winter bean height by stage 5 (ripening) measured here is 1.2 m (Figure 5) which is similar to a plant height of 1.12 m for Tundra winter bean reported by PGRO (3) and within the range to be expected due to differences in winter bean plant height will vary depending on geographical location, climate conditions, soil type and fertiliser and other treatment variations.

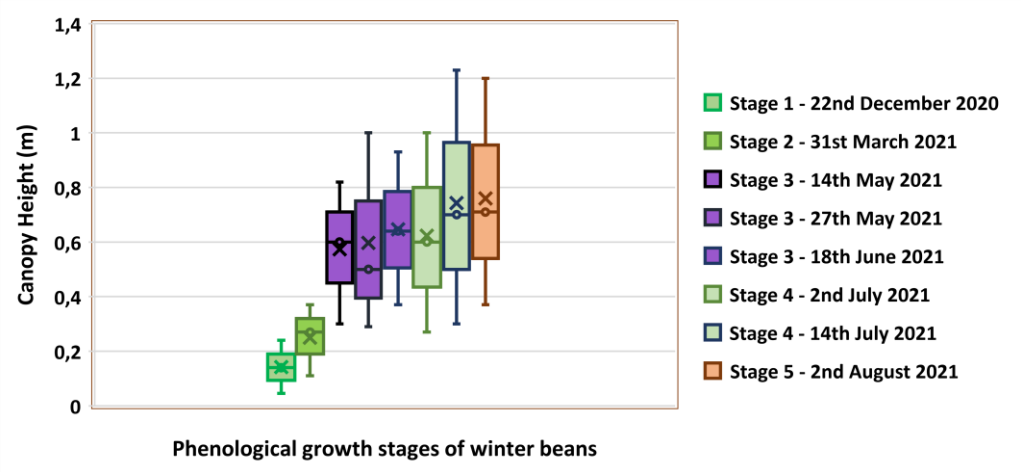


Note: The limits of the box represent the upper and lower quartile of the data as assessed at the 95% confidence limit while the whiskers show the minimum and maximum heights determined. The horizontal line within the box represents the median height while the cross is the mean height.

Figure 5. Winter bean canopy height at phenological growth stages.

### *Prediction of seed yield*

Initially, two dates in May 2021 (14 and 27 May) were chosen to estimate seed yield during the growing peak period (Stage 3, flowering) of the winter bean crop. The vegetation index maps were classified into six clusters by iso-cluster classification. The classified clusters were grouped as soil surface, grassland or shrub, and a healthy winter bean crop (Figure 6). The healthy winter bean crop had an average NDVI value of 0.5, a GNDVI value of 0.41 and an NDRE value of 0.45. These are considered moderate values for a crop but accurately portray the sparse nature of the winter bean crop across the High Dowell field (Figure 6(a)). Generally, higher values of NDVI, GNDVI and NDRE (typically between 0.6 to 1) are found in dense vegetation due to the high levels of chlorophyll. The final seed yield of the winter bean crop was estimated by calculating the pixel areas of healthy vegetation within the crop classified by iso-cluster classification using NDVI, GNDVI and NDRE vegetation index maps (Figure 6). The NDVI iso-cluster classified image (Figure 6(b)) shows a better classification for the winter bean crop vegetation from the surrounding grassland or shrub and soils surfaces in comparison to the GNDVI and NDRE (Figure 6(c) and 6(d)) iso-cluster classified images. NDVI works well for determining the vegetation of crop in less dense biomass and in early to mid-development stages of a crop (8).

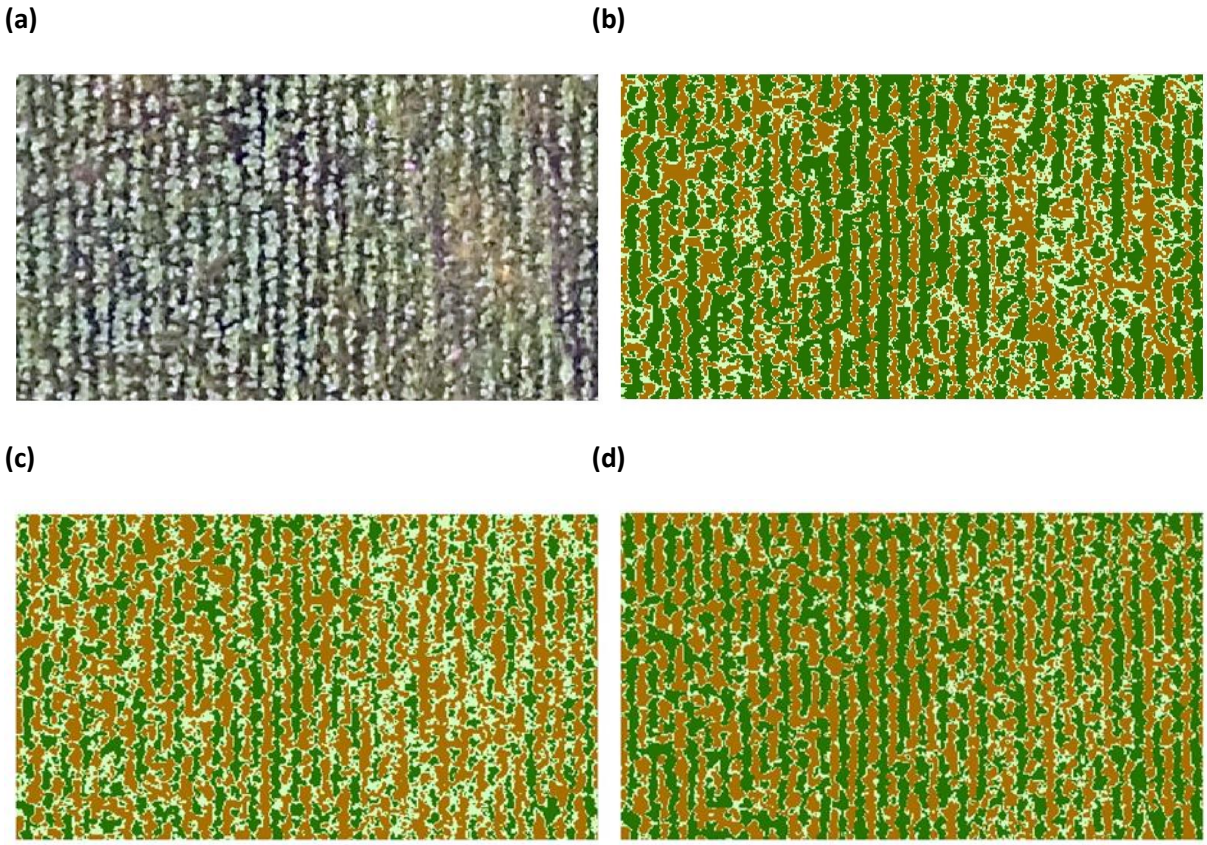


Figure 6. (a) RGB image (b) NDVI iso-clustered image (c) GNDVI iso-clustered image (d) NDRE iso-clustered image. Note for (b)-(d): Dark green represents healthy winter bean crop. Light green represents grasslands or shrubs. Brown represents soil surface.

The comparison between the estimated yield by NDVI and the actual seed yields within the High Dowell site is shown in Figure 4 using the FarmTRX clusters i.e. A = low yield (mean 1.15 t/ha), B = medium yield (mean 1.28 t/ha), C = high yield (mean 1.38 t/ha), and D = very high yield (mean >1.57 t/ha). A strong correlation is noted between the estimated and actual seed yields across the two days investigated in May 2021 (Figure 7) in many pairs of data, with NDVI being generally more strongly correlated than GNDVI or NRDE in almost every case. The correlation coefficient and RMSE by NDVI for the 14 May was an $R^2$ of 0.84 with an RMSE of 0.32 (Figure 7(a)) and for the 27 May was an $R^2$ of 0.87 with an RMSE of 0.53 (Figure 7(b)). Whereas the estimated yield by GNDVI and NDRE was significantly lower and showed weak correlation between the estimated and actual seed yield (Figure 8 and 9). The correlation coefficient and RMSE from GNDVI for the 14 May was $R^2 = 0.66$ with an RMSE of 0.92 (Figure 8(a)), whilst from the 27 May was R2 = 0.66 with an RMSE of 0.57 (Figure 8(b)). For the NDRE, the correlation coefficient for the 14 May was $R^2 = 0.55$ with an RMSE of 0.42 (Figure 9(a)) and for the 27 May the $R^2$ was 0.7 with an RMSE of 0.62 (Figure 9(b)).

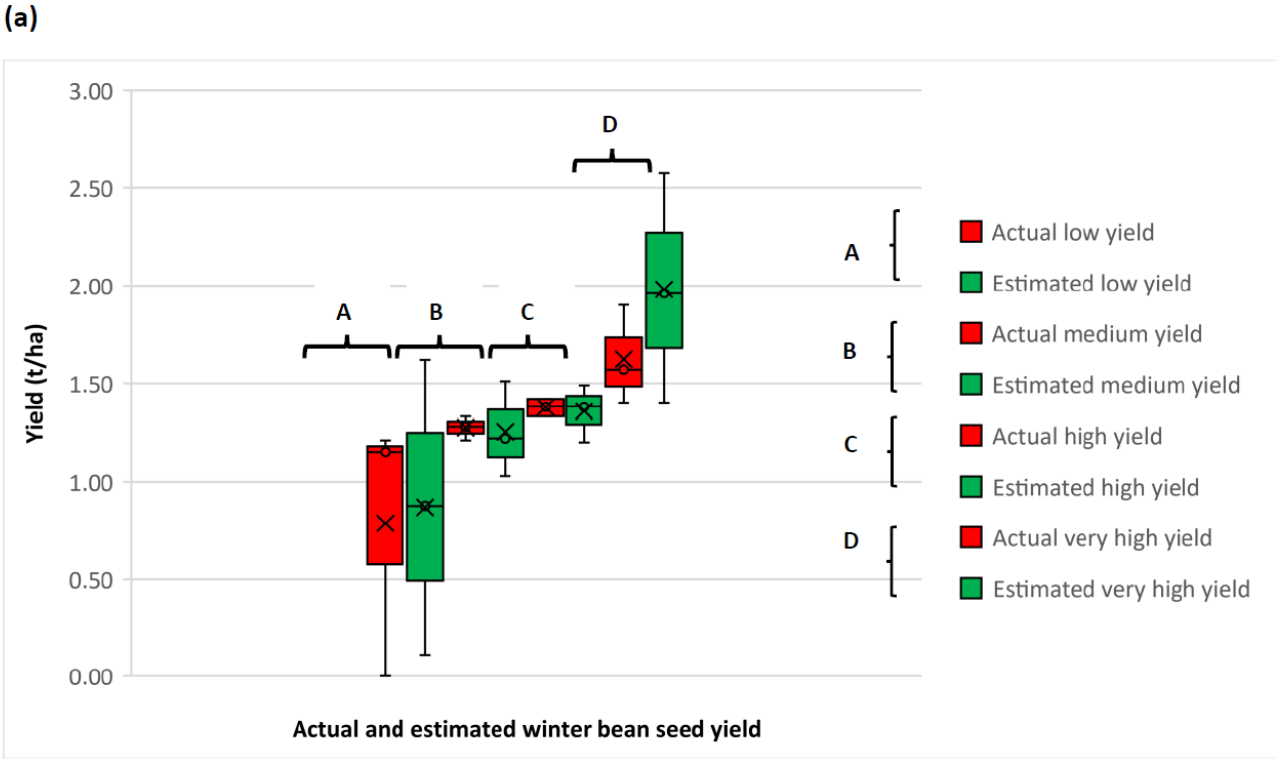


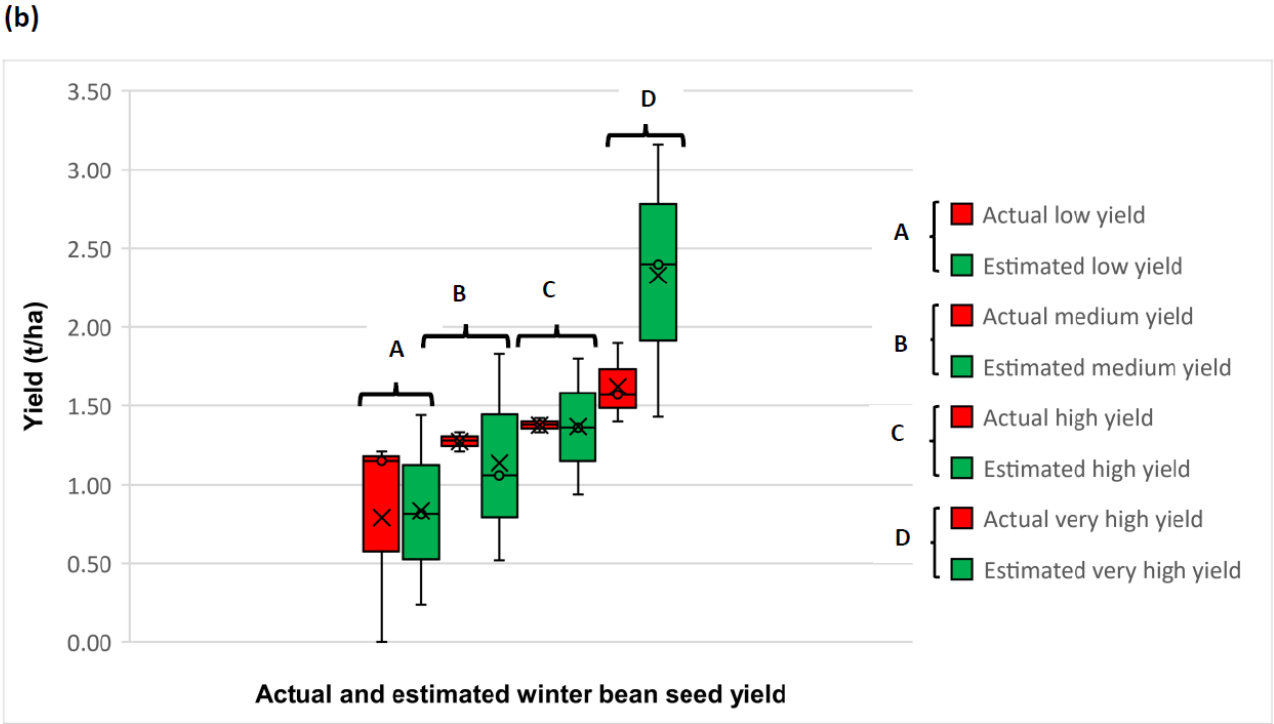


Figure 7. (a) Comparison between actual and estimated winter bean yield by NDVI on (a) 14 May 2021, and (b) 27 May 2021.
[Correlation coefficient and RMSE for 14 May 2021 ($R^2$ = 0.84 and RMSE = 0.32) and 27 May 2021 ($R^2$ = 0.87 and RMSE = 0.53)]

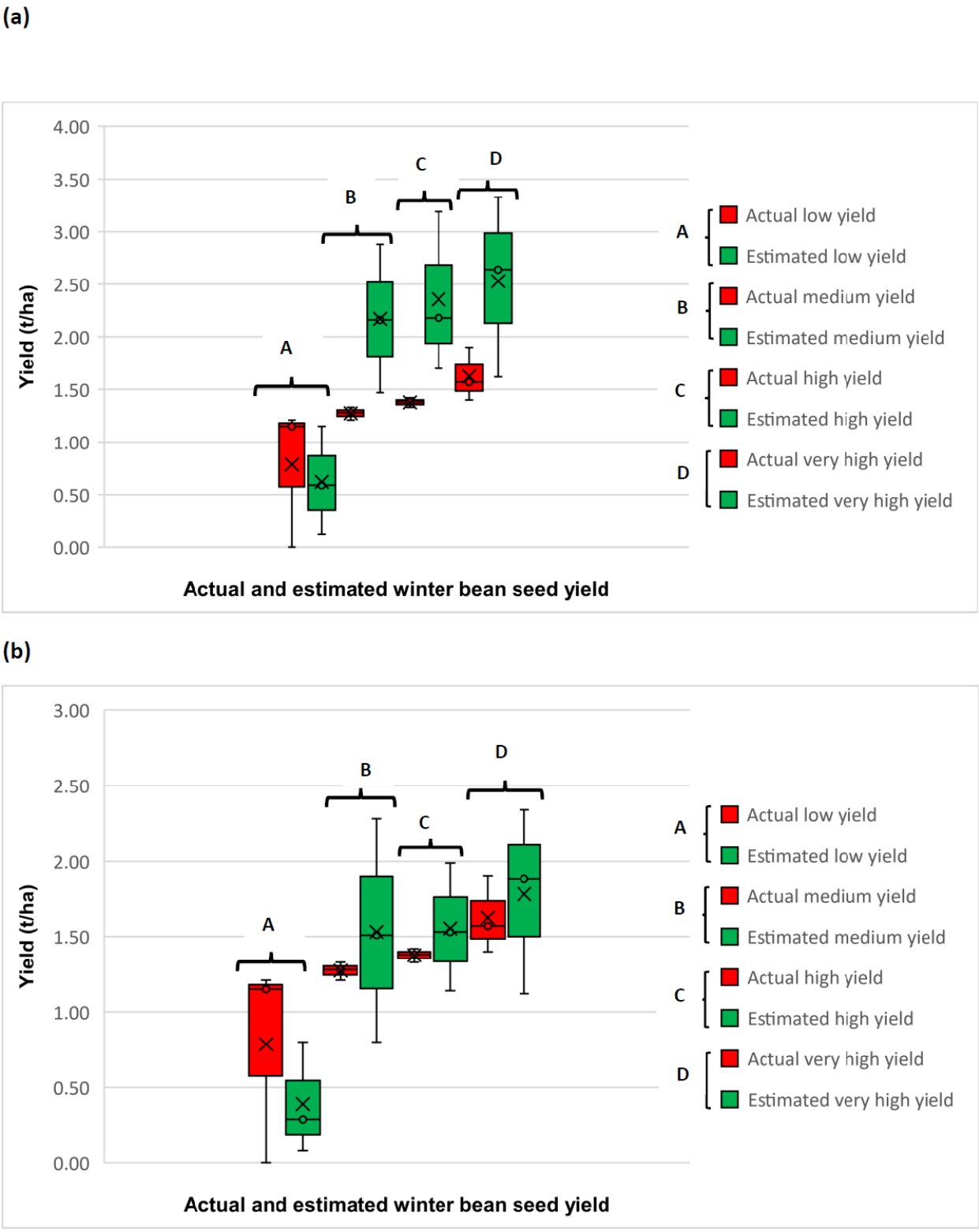


Figure 8. (a) Comparison between actual and estimated winter bean seed yield by GNDVI on (a) 14 May 2021, and (b) 27 May 2021.
[Correlation coefficient and RMSE for 14 May 2021 ($R^2$ = 0.66 and RMSE = 0.92) and 27 May 2021 ($R^2$ = 0.66 and RMSE = 0.57)]

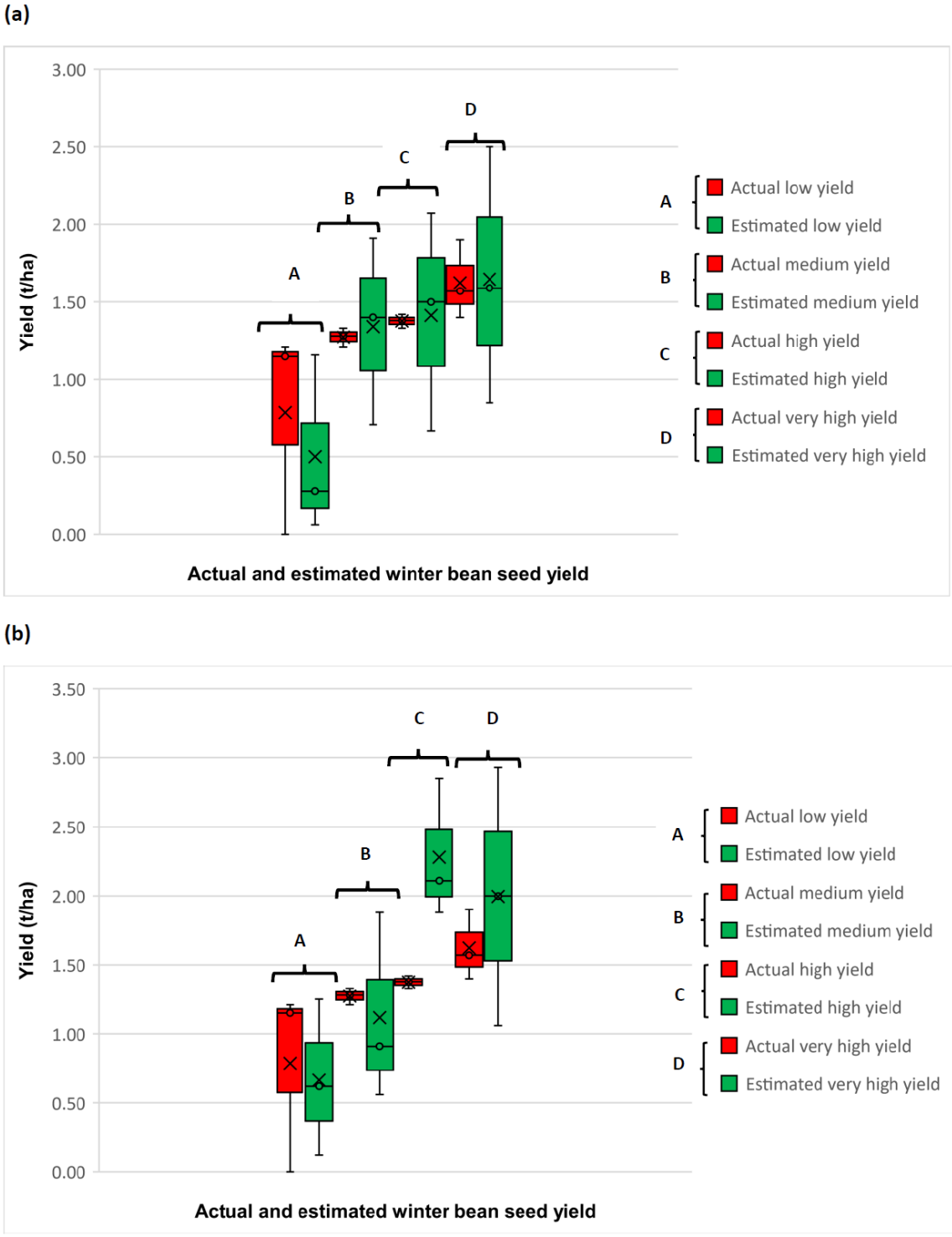


Figure 9. (a) Comparison between actual and estimated winter bean seed yield by NDRE on (a) 14 May 2021, and (b) 27 May 2021.
[Correlation coefficient and RMSE for 14 May 2021 ($R^2$ = 0.55 and RMSE = 0.42) and 27 May 2021 (R2 = 0.70 and RMSE = 0.62)]

However, NDRE did show better performance as a predictor for the highest crop yields. For very high yield area (D in Figure 4) the estimated yield by NDRE

was significantly better than the estimated NDVI (Figure 9(a) and 9(b)). A similar observation was observed for the high yield area (D in Figure 4) estimated by GNDVI on 27 May (Figure 8(b)). These data support the conclusion that NDRE will be more sensitive and hence provide better indicators of yield for crops with dense vegetation in their later growth stages that have accumulated high levels of chlorophyll in their leaves. In contrast, NDVI has shown to be a better indicator of vegetation for a crop with sparse vegetation i.e. winter beans.

## Conclusion

This research has shown that a canopy height model, resultant from UAV-MSI data, can effectively predict the crop height of winter beans over the phenological growth stages (9 months). Secondly, the study demonstrates a simple and effective method for estimating winter bean seed yield at the flowering stage (Stage 3 in the phenological growth stages) 3 months prior to harvesting, using three different vegetation indices. Thirdly, the estimation of winter bean yield across the phenological growth stages is highlighted. Finally, NDVI has been shown to be a good estimator of winter bean yield, due to its sparse vegetation. Therefore, this new approach for winter beans can provide insights to the farmer, and agronomist, in terms of crop development, as well as estimate the final seed yield in advance of its ripening and harvesting using a direct, automated approach with commercially available software that does not require challenging coding.

## Acknowledgements

Access to visit and monitor the farm at Kiln Pitt Hill, Consett DH8 9SL, was granted by John Miller and family (T & AE Miller). In addition, we acknowledge the input from Stephen Brown for information on the agricultural site investigated.

## References

1.LGSeedUK,https://www.arablescotland.org.uk/sites/www.arablescotland.org.uk/files/2020-06/Tundra%20Winter%20Bean%20Technical%20Summary.pdf, (accessed September 2022).

2.Senova,https://irp.cdnwebsite.com/55da3d94/files/uploaded/Winter%20Bean%20Growers%20Guide%20060422.pdf, (accessed September 2022).

3.Nickerson, https://www.nickersonseeds.co.uk/products/pulses/tundra/data-sheet/, (accessed September 2022).

4.Farmers Weekly, Disease alert for winter beans after mild winter - Farmers Weekly (fwi.co.uk) (accessed September 2022).

5.GrowNotes, https://grdc.com.au/resources-and-publications/grownotes/crop-agronomy/faba-bean-southern-region-grownotes/GrowNote-Faba-South-5-Plant-Growth-Physiology.pdf, (accessed September 2022).

6.Jimenez-Berni JA, Deery DM, Rozas-Larraondo P, Condon ATG, Rebetzke GJ, James RA, et al. High Throughput Determination of Plant Height, Ground Cover, and Above-Ground Biomass in Wheat with LiDAR. Front Plant Sci. 2018;9:237. doi:10.3389/fpls.2018.00237

7.Mulla DJ. Twenty five years of remote sensing in precision agriculture: Key advances and remaining knowledge gaps. Biosystems Engineering. 2013;114(4):358-71. doi:10.1016/j.biosystemseng.2012.08.009

8.Sishodia RP, Ray RL, Singh SK. Applications of Remote Sensing in Precision Agriculture: A Review. Remote Sensing. 2020;12(19). doi:10.3390/rs12193136

9.Ji Y, Chen Z, Cheng Q, Liu R, Li M, Yan X, et al. Estimation of plant height and yield based on UAV imagery in faba bean (Vicia faba L.). Plant Methods. 2022;18(1):26. doi:10.1186/s13007-022-00861-7

10.Alabi TR, Abebe AT, Chigeza G, Fowobaje KR. Estimation of soybean grain yield from multispectral high-resolution UAV data with machine learning models in West Africa. Remote Sensing Applications: Society and Environment. 2022;27. doi:10.1016/j.rsase.2022.100782

11.Maimaitijiang M, Sagan V, Sidike P, Hartling S, Esposito F, Fritschi FB. Soybean yield prediction from UAV using multimodal data fusion and deep learning. Remote Sensing of Environment. 2020;237. doi:10.1016/j.rse.2019.111599

12.Boiarskii B. Comparison of NDVI and NDRE Indices to Detect Differences in Vegetation and Chlorophyll Content. Journal of Mechanics of Continua and Mathematical Sciences. 2019;spl1(4). doi:10.26782/jmcms.spl.4/2019.11.00003

13.Shirsath PB, Sehgal VK, Aggarwal PK. Downscaling regional crop yields to local scale using remote sensing. Agriculture. 2020;10(58):2-14. doi:10.3390/agriculture10030058

14.Xie T, Li J, Yang C, Jiang Z, Chen Y, Guo L, et al. Crop height estimation based on UAV images: Methods, errors, and strategies. Computers and Electronics in Agriculture. 2021;185. doi:10.1016/j.compag.2021.106155

15.Rouse Jr JW, Haas RH, Schell JA, Deering DW. Monitoring vegetation systems in the Great Plains with ERTS. Third Earth Resources Technology Satellite-1 Symposium: Volume 1; Technical presentations, section B, SC Freden, EP Mercanti, and MA Becker, Eds., NASA Special Publ. InConference Proceedings, Document ID: 19740022592 1974 (pp. 1-9).

16.Gitelson AA, Kaufman YJ, Merzlyak MN. Use of a green channel in remote sensing of global vegetation from EOS-MODIS. Remote sensing of Environment. 1996 Dec 1;58(3):289-98. https://doi.org/10.1016/S0034-4257(96)00072-7

17.Sims DA, Gamon JA. Relationships between leaf pigment content and spectral reflectance across a wide range of species, leaf structures and developmental stages. Remote sensing of environment. 2002 Aug 1;81(2-3):337-54. http://dx.doi.org/10.1016/S0034-4257(02)00010-X